TOMOGRAPHY® RESEARCH ARTICLE

Enhanced Bone Metastases in Skeletally Immature Mice

Henry R. Haley[1], Nathan Shen[1], Tonela Qyli[1], Johanna M. Buschhaus[1,2], Matthew Pirone[1], Kathryn E. Luker[1], and Gary D. Luker[1,2,3]

[1]Departments of Radiology; [2]Biomedical Engineering; and [3]Microbiology and Immunology, University of Michigan Medical School, Ann Arbor, MI

Corresponding Author:
Gary D. Luker, MD
University of Michigan Medical School, 109 Zina Pitcher Place, A524
BSRB, Ann Arbor, MI 48109-2200;
E-mail: gluker@umich.edu

Key Words: breast cancer, bone metastasis, computed tomography, bioluminescence imaging
Abbreviations: Computed tomography (CT)

ABSTRACT

Bone constitutes the most common site of breast cancer metastases either at time of presentation or recurrent disease years after seemingly successful therapy. Bone metastases cause substantial morbidity, including life-threatening spinal cord compression and hypercalcemia. Given the high prevalence of patients with breast cancer, health-care costs of bone metastases (>$20,000 per episode) impose a tremendous economic burden on society. To investigate mechanisms of bone metastasis, we developed femoral artery injection of cancer cells as a physiologically relevant model of bone metastasis. Comparing young (~6 weeks), skeletally immature mice to old (~6 months) female mice with closed physes (growth plates), we showed significantly greater progression of osteolytic metastases in young animals. Bone destruction increased in the old mice following ovariectomy, emphasizing the pathologic consequences of greater bone turnover and net loss. Despite uniform initial distribution of breast cancer cells throughout the hind limb after femoral artery injection, we observed preferential formation of osteolytic bone metastases in the proximal tibia. Tropism for the proximal tibia arises in part because of TGF-β, a cytokine abundant in both physes of skeletally immature mice and matrix of bone in mice of all ages. We also showed that age-dependent effects on osteolytic bone metastases did not occur in male mice with disseminated breast cancer cells in bone. These studies establish a model system to specifically focus on pathophysiology and treatment of bone metastases and underscore the need to match biologic variables in the model to relevant subsets of patients with breast cancer.

INTRODUCTION

Metastatic breast cancer currently affects >150,000 women in the United States, three-fourths of whom initially presented with local or regional disease (1). Breast cancer most commonly metastasizes to bone, occurring in 80% of patients with metastatic disease in any site. Bone metastases cause substantial morbidity, including severe pain, instability, and pathologic fracture, complications that markedly impair quality of life in affected patients. Breast cancer metastases in bone may also cause acute life-threatening conditions such as spinal cord compression and malignant hypercalcemia. Once breast cancer metastasizes to bone or other sites, prognosis drops dramatically. Patients with local or regional disease have a 5-year survival rate of >90% or 70%, respectively, while for those with metastatic breast cancer, survival plummets to 20%–30% (2). These facts underscore the need for mechanistic studies in physiologically relevant model systems to ultimately prevent and/or more effectively treat breast cancer metastasis to bone.

Although breast cancer most commonly affects older women with median age of 62 years at diagnosis, studies of breast cancer metastasis to bone typically use young (~6- to 8-week-old; 3) female mice. Unlike humans, mice at this age remain skeletally immature with open physes (growth plates) in long bones of extremities. Physes concentrate numerous growth factors and cytokines that promote bone growth and remodeling, including TGF-β (transforming growth factor beta-1), fibroblast growth factors, bone morphogenetic proteins, and Indian hedgehog (4). In further contrast with humans, mice also experience increase in bone mass after puberty (5). This difference between rodents and humans is exacerbated by the fact that osteoporosis, a condition marked by increased bone remodeling and overall loss of bone density, occurs in 30% of postmenopausal women, the group at the highest risk for breast cancer (6). Because breast cancer occurs in skeletally mature persons who also commonly have osteoporosis, studies on bone metastases in skeletally immature mice provide an abundance and range of skeletal growth factors not present in patients.

Experimental models of bone metastasis in mice commonly rely on intracardiac injection of cancer cells into the left ventricle or direct injection into bone. While intracardiac injection

ISSN 2379-1381 http://dx.doi.org/10.18383/j.tom.2018.00010

mimics hematogenous dissemination of cancer cells to bone, this approach generates widespread metastases to multiple organs unless investigators select clones with particular tropism for bone (7-9). Therefore, mice typically must be euthanized for humane endpoints before progression of bone changes, which also minimizes opportunities to investigate bone-targeted therapies. Direct intraosseous injection of cancer cells eliminates problems of widespread metastasis, allowing studies to focus on the bone environment in metastasis. However, this experimental method introduces cancer cells into nonphysiological niches that may not be relevant to hematogenous spread of metastasis in breast cancer and other solid tumors (7, 8).

To selectively produce experimental, hematogenous bone metastases in mice, Wang et al. recently developed a model based on direct injection of cancer cells into the iliac artery of mice (9). While technically challenging, this approach consistently delivers cancer cells into the circulation, enabling cells to access physiologically relevant niches in lower extremity bone marrow without metastases in other sites. We modified this method to inject cancer cells into the femoral artery of mice, a site we found to be more accessible and reproducible, and then used this model system to investigate the effects of age, gender, and bone remodeling on osteolytic breast cancer metastases. We discovered that young female mice experience greater extent and progression of osteolytic bone metastases than older (~6-month-old) mice. Inhibiting TGF-β reduced bone metastases in young female mice, while older females became more susceptible to osteolytic bone lesions after ovariectomy was performed to produce a postmenopausal state. Interestingly, male mice did not exhibit age-dependent differences, as both young and old mice showed comparable, minimal bone destruction. These results highlight age- and gender-dependent differences in breast cancer metastases to bone, underscoring the need to match the clinical patient population to physiologically appropriate models.

MATERIALS AND METHODS

1. Cells: We cultured AT-3 C57BL/6J murine breast cancer cells stably expressing firefly luciferase (AT3-FL) as described previously (10).
2. Mice: We originally purchased C57BL/6J mice (stock number 000664) from the Jackson Laboratory (Bar Harbor, ME) and subsequently bred mice at the University of Michigan.
3. Femoral artery injection of cancer cells: The University of Michigan IACUC approved all animal procedures under protocol 00006795. For these experiments, we used 6- to 7-week-old, skeletally immature mice ("young") or 31- to 60-week-old skeletally mature female or male animals ("old") as noted in each figure. To inject breast cancer cells via the femoral artery, we shaved and applied a topical depilatory agent to the left hind limb. We anesthetized mice with 1%-2% isoflurane throughout the procedure. Using sterile technique, we incised skin over the left femoral artery and then used a stereomicroscope to direct blunt dissection of this blood vessel. We injected 1×10^5 AT3-FL cells in 20 μL of 0.9% NaCl into the femoral artery through a 31-gauge needle. The injected solution contained 1% trypan blue to verify injection into the artery. After achieving hemostasis through direct pressure on the artery with a sterile cotton swab, we closed the incision with nonresorbable suture (PROLENE 4-0 FS-2). In selected experiments, we performed bioluminescence imaging within 10 to 15 min of injection, analyzing immediate distribution of injected cells in euthanized mice as we have described (11).
4. Ovariectomy: We removed the ovaries from skeletally mature female c57BL/6 mice as described (12).
5. Bioluminescence imaging: We performed bioluminescence imaging at times indicated in figure legends as described previously (13). We presented data as mean values for photon flux $\pm$ SEM.
6. Computed tomography (CT): We imaged hind limbs of anesthetized mice by CT (Bruker SkyScan 1176) before injection of cancer cells and then at times indicated in figures to detect osteolytic metastases. We used the following parameters: 70 kV, 35-μm pixel size, and 1-mm aluminum filter. We acquired 2 scans, averaging 3 frames for each position. Scans required ~9 min and used a dynamic range of 0–0.035. We quantified bone loss using algorithms developed in Matlab (MathWorks, Natick, MA) to measure total volume of the proximal tibia at each time point (14). We normalized this value to 0% bone destruction before injection of cancer cells for each mouse. We also enumerated mice with detectable bone metastases at each time point.
7. Inhibition of TGF-β signaling in mice: We pretreated mice with 60 mg/kg TGF-β receptor I kinase inhibitor, SD-208 (Selleckchem, Houston, TX) for 2 days before injecting breast cancer cells and then continued treatment by daily oral gavage until we euthanized mice for tumor burden. We formulated a 20 mM stock solution of SD-208 in 1% methylcellulose by stirring overnight at 4°C. We warmed the compound to room temperature before administering to mice (15).
8. Immunostaining: We decalcified femur and tibia of mice by standard methods and prepared formalin-fixed, paraffin-embedded sections (University of Michigan ULAM Histology Core). After deparaffinization, rehydration of sections, and wet autoclave antigen retrieval, we stained sections for phosphorylated SMAD2 as a marker of active TGF-β signaling (1:50 dilution of anti-pSMAD2 antibody LS-C199582, LSBio, Seattle, WA) and Cy3 fluorescent secondary antibody (1:400 dilution, Code Number: 711-165-152, Jackson ImmunoResearch, West Grove, PA). We counterstained sections with DAPI to detect nucleated cells.
9. Statistics: We compared groups by t test (GraphPad Prism version 7.0, La Jolla, CA), defining significant differences as $P < .05$.

RESULTS

Breast Cancer Cells Injected via the Femoral Artery Distribute Uniformly in Tibia but Produce Only Proximal Osteolytic Metastases

As we initially developed our method of femoral artery injection of cancer cells in young (~6- to 8-week-old mice), we observed that mice invariably developed osteolytic bone metastases in the proximal tibia (Figure 1, A and B). We noted a similar preference for the proximal tibia in multiple publications on bone metastases in mice from both iliac artery and intracardiac injections

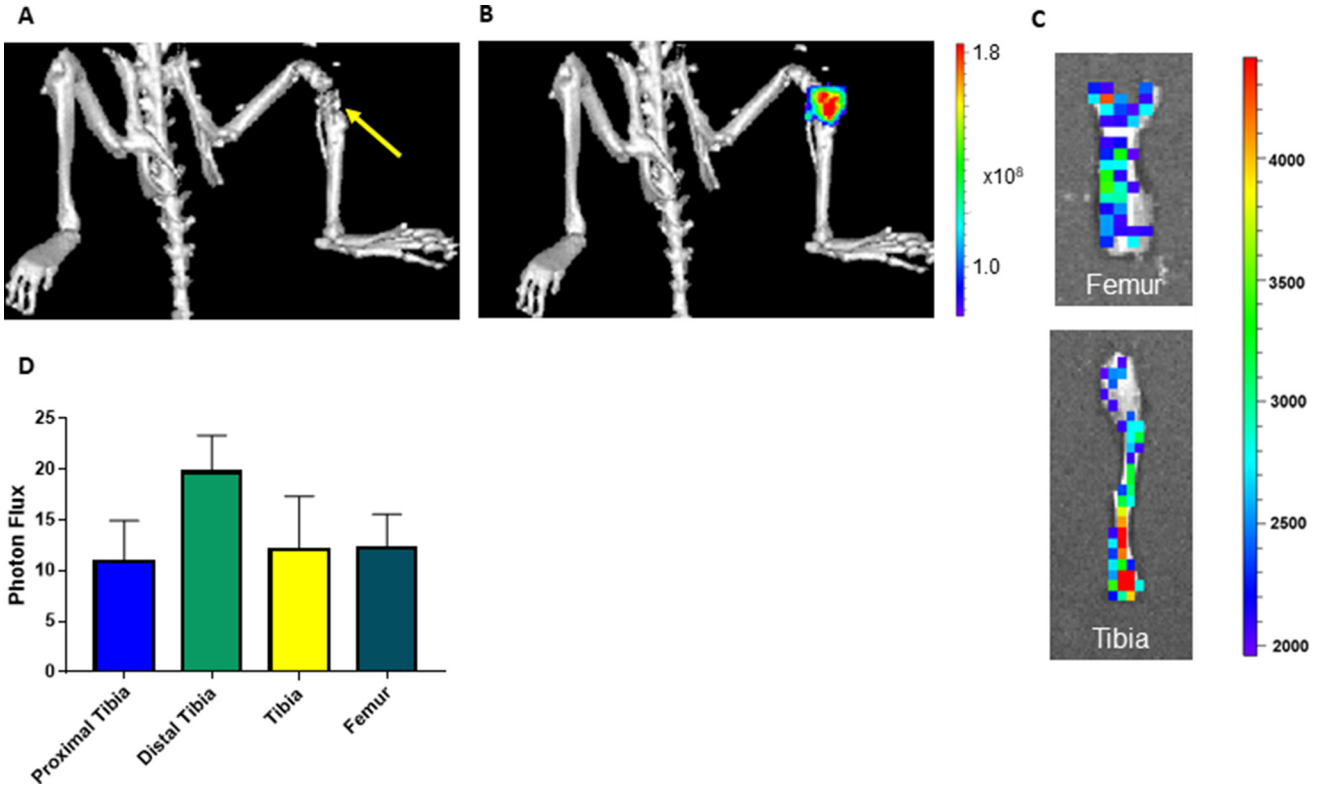

Figure 1. Osteolytic metastases preferentially occur in the proximal tibia. Representative computed tomography (CT) (A) and merged bioluminescence/CT (B) images of an osteolytic lesion produced by mouse AT-3-FL breast cancer cells 21 days after injection via the left femoral artery. The yellow arrow in (A) shows the osteolytic metastasis in the proximal tibia. Ex vivo bioluminescence image shows uniform distribution of AT-3-FL cells in femur and tibia of a mouse ~10 to 15 min after femoral artery injection (C). The scale bar shows a range of colors for pseudocolor display of photon flux values, with red and blue defining the highest and lowest values, respectively. The graph displays mean values for photon flux + SEM (n = 4 mice) for initial localization of cancer cells in the proximal and distal tibia and overall tibia and femur as shown in (C) (D).

performed in young animals (16-18). To ensure our method did not preferentially disseminate injected cells only to the proximal tibia, we investigated initial distribution of breast cancer cells following femoral artery injection. We injected young mice with AT3-FL breast cancer cells via the femoral artery, then injected luciferin, and then euthanized mice 10–15 min after injection of cancer cells. Bioluminescence images of dissected femur and tibia of mice showed uniform initial distribution of breast cancer cells in the femur. While imaging showed a trend for higher initial signal from breast cancer cells in the distal tibia, differences between proximal and distal portions of this bone were not significant (Figure 1, C and D). These data established that preferential growth of AT-3 breast cancer cells and osteolytic metastases in the proximal tibia occurred because this site provides a local environment favoring growth of breast cancer cells arriving at that site.

Accelerated Bone Metastases in Skeletally Immature Female Mice

To investigate age-dependent effects on the growth of disseminated tumor cells in bone marrow and progression to osteolytic metastases, we introduced AT3-FL breast cancer cells via femoral artery injection into 6- to 7-week-old (young) and 31- to 47-month-old female C57BL/6J mice. Although bioluminescence imaging showed a trend toward greater overall proliferation of AT3-FL breast cancer cells in young mice, these differences did not reach statistical significance as defined by $P < .05$ (Figure 2, A and B). By comparison, osteolytic lesions developed earlier and to a greater extent in young mice. Twelve days after injection, CT revealed osteolytic lesions in the proximal tibia of 3 of 5 young mice as compared with 1 of 5 old mice (Table 1). All young mice developed osteolytic lesions in proximal tibia 25 days after injection of AT3-FL breast cancer cells with a significantly greater extent of bone destruction than old mice ($P < .05$) (Fig 2, C and D). Young mice lost ~50% of bone volume in the proximal tibia measured by CT, whereas bone volume decreased by only 15% in old mice.

TGF-β is one of the major cytokines present in the physis of mice, where this molecule regulates bone growth, formation, and remodeling (19). Because TGF-β has also been linked closely to bone metastasis in breast cancer and other malignancies, we

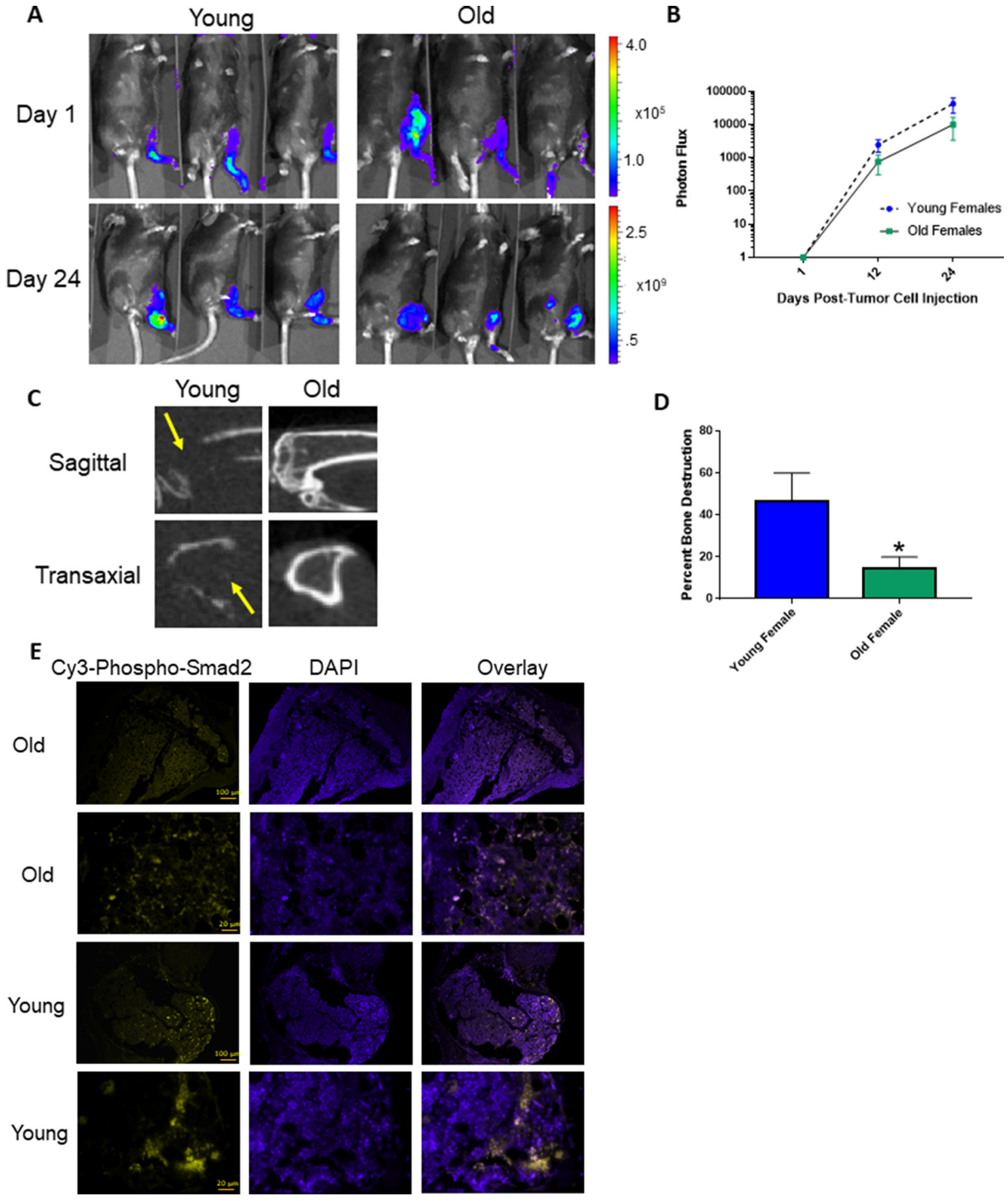

Figure 2. Enhanced osteolytic lesions in skeletally immature female mice. Bioluminescence images of representative young (6–7 weeks) versus old (31–47 weeks) female mice 1 day and 24 days after injection of AT-3-FL cells via the left femoral artery. The scale bar shows the pseudocolor display for photon flux values (A). The graph displays mean ± SEM for quantified bioluminescence data for the growth of breast cancer cells in the left hind limbs of mice in (A) (n = 4 per group). We detected no significant difference in tumor growth between young and old female mice (B). Representative sagittal and transaxial CT images of proximal tibias from skeletally immature young and skeletally mature old mice at the time of euthanization on day 25. Arrows show large osteolytic lesion destroying the proximal tibia of the young mouse (C). The graph shows mean values + SEM for percent bone destruction in proximal tibias of mice normalized to 0% before injection of cancer cells (day 0) (* denotes $P < .05$) (D). Representative immunofluorescence images of phosphorylated Smad2 staining as a marker of active TGF-β signaling show enhanced staining in the proximal tibia of young mice (E). DAPI staining depicts nucleated cells. Overlay shows active TGF-β signaling corresponds with nucleated cells. Scale bar are as noted on images.

Table 1. Mice With Osteolytic Lesions Identified by Micro-CT

	Day 1	Day 12	Day 25
Young Female Mice	0	3/5	4/4
Old Female Mice	0	1/5	4/5

hypothesized that TGF-β signaling contributes to differences in osteolytic metastases in young versus old female mice (20). We analyzed proximal tibias of young and old mice for TGF-β signaling on the basis of phosphorylation of SMAD2 (p-SMAD2), a kinase substrate of activated TGF-β receptor I (TGF-βRI) (21). Immunofluorescence staining revealed greater amounts of p-SMAD2 in young mice (Figure 2E). Overall, these data show greater susceptibility of young mice to osteolytic breast cancer metastases and highlight differences in TGF-β signaling as one potential mechanism.

Inhibiting TGF-β Signaling Reduces Osteolytic Bone Lesions in Young Mice

To directly test the hypothesis that TGF-β signaling promotes bone metastasis in young mice, we treated young (6-week-old) female mice daily with 60 mg/kg SD-208, a selective inhibitor of TGF-βRI or vehicle control (1% methylcellulose) (21). We initiated treatment 2 days before femoral artery injection of AT3-FL breast cancer cells and continued daily dosing through the end of the experiment. Bioluminescence imaging showed essentially identical growth of breast cancer cells in both groups, showing that SD-208 did not directly affect proliferation of AT3-FL cells in the bone marrow (Figure 3, A and B). CT performed 19 days after injection of breast cancer cells showed osteolytic lesions in the metaphysis of mice treated with vehicle control, resulting in loss of ~14% of bone volume (Figure 3, C and D). By comparison, treatment with SD-208 almost completely blocked osteolytic lesions in young mice ($P < .05$).

We analyzed inhibition of TGF-β signaling by immunofluorescence staining for p-SMAD2. Young female mice treated with vehicle control showed abundant p-SMAD2 in proximal tibia, verifying high activity of TGF-β signaling near the physis in the setting of bone metastasis (Figure 3E). By comparison, treatment with SD-208 markedly reduced p-SMAD2, establishing that this compound blocked TGF-β signaling as expected. The ability to almost completely eliminate osteolytic bone metastases in young female mice by blocking TGF-βRI strongly implicates TGF-β signaling as a key driver of differences in disease progression in young versus old female mice.

Minimal, Age-Independent Osteolytic Metastases in Male Mice

Because 1% of breast cancers occur in men, we compared proliferation of breast cancer cells and formation of osteolytic metastases in young versus old male mice after femoral artery injection of AT3-FL cells. Similar to results in female mice, we did not detect significant differences in the growth of breast cancer cells in the lower extremities of young versus old mice (Figure 4, A and B). Strikingly, very minimal bone destruction occurred in either group. Twenty days after injection of breast cancer cells, young and old male mice lost only 6% and 1% of bone volume in the proximal tibia (Figure 4, C and D). These small losses in bone volume did not differ significantly between groups, showing that age-dependent effects on osteolytic breast cancer metastases happen in only female mice in this model system.

Ovariectomy Increases Osteolytic Lesions in Older Mice

Breast cancer metastases present most commonly in postmenopausal women. Loss of estrogen in this population leads to enhanced activity of osteoclasts with associated bone remodeling and degradation, a condition we hypothesized would increase osteolytic metastases in older female mice. We removed ovaries from older mice to experimentally induce menopause and waited an additional 5 weeks after ovariectomy before injecting AT3-FL breast cancer cells through the femoral artery. As a control group, we used age-matched (58- to 60-week-old) female mice who underwent sham ovariectomy. Both groups of mice showed comparable growth of AT3-FL cells in the lower extremities as measured by bioluminescence imaging (Figure 5, A and B). CT scans of the hind limb showed earlier appearance of osteolytic bone metastases in the ovarietomy group with visible lesions evident by day 13 (Figure 5, C and D). Osteolytic lesions eventually developed in both groups of mice by day 23, although the extent of bone destruction remained greater in the ovariectomy group. Area-under-the-curve analysis of tibial bone destruction over the full-time course of the study highlighted effects of ovariectomy to accelerate progression of osteolytic metastases in old mice (Figure 5E).

DISCUSSION

While coordinated functions of osteoblasts and osteoclasts actively remodel bone throughout life, bone turnover accelerates during periods of skeletal growth and loss of anabolic bone hormones such as estrogen or androgens. Our study reveals that environmental conditions promoting enhanced bone turnover and remodeling dramatically regulate progression of osteolytic bone metastases in breast cancer. Using a novel experimental model to selectively produce bone metastases through injection of cancer cells into the femoral artery, we showed accelerated formation and progression of osteolytic lesions in younger (6–8 weeks), skeletally immature mice relative to older (≥31 weeks) mice with closed physes. These differences occurred without significant differences in proliferation of breast cancer cells in bone/bone marrow as measured by imaging, underscoring age-dependent effects of the tumor environment on osteolytic lesions. We note the vast majority of studies of breast cancer bone metastasis rely exclusively on younger mice, a model system that fails to recapitulate almost exclusive occurrence of breast cancer in skeletally mature adults. Studies with younger mice avoid costs of housing mice for extended periods of time but may yield conclusions about mechanisms of bone metastasis that do not exist in patients with breast cancer. This discordance potentially contributes to ongoing challenges translating promising results in animal models to successful therapies (22). Our observed differences in osteolytic breast cancer metastases between younger and older mice are comparable to those reported previously between 6- and 16-week-old mice with an intracar-

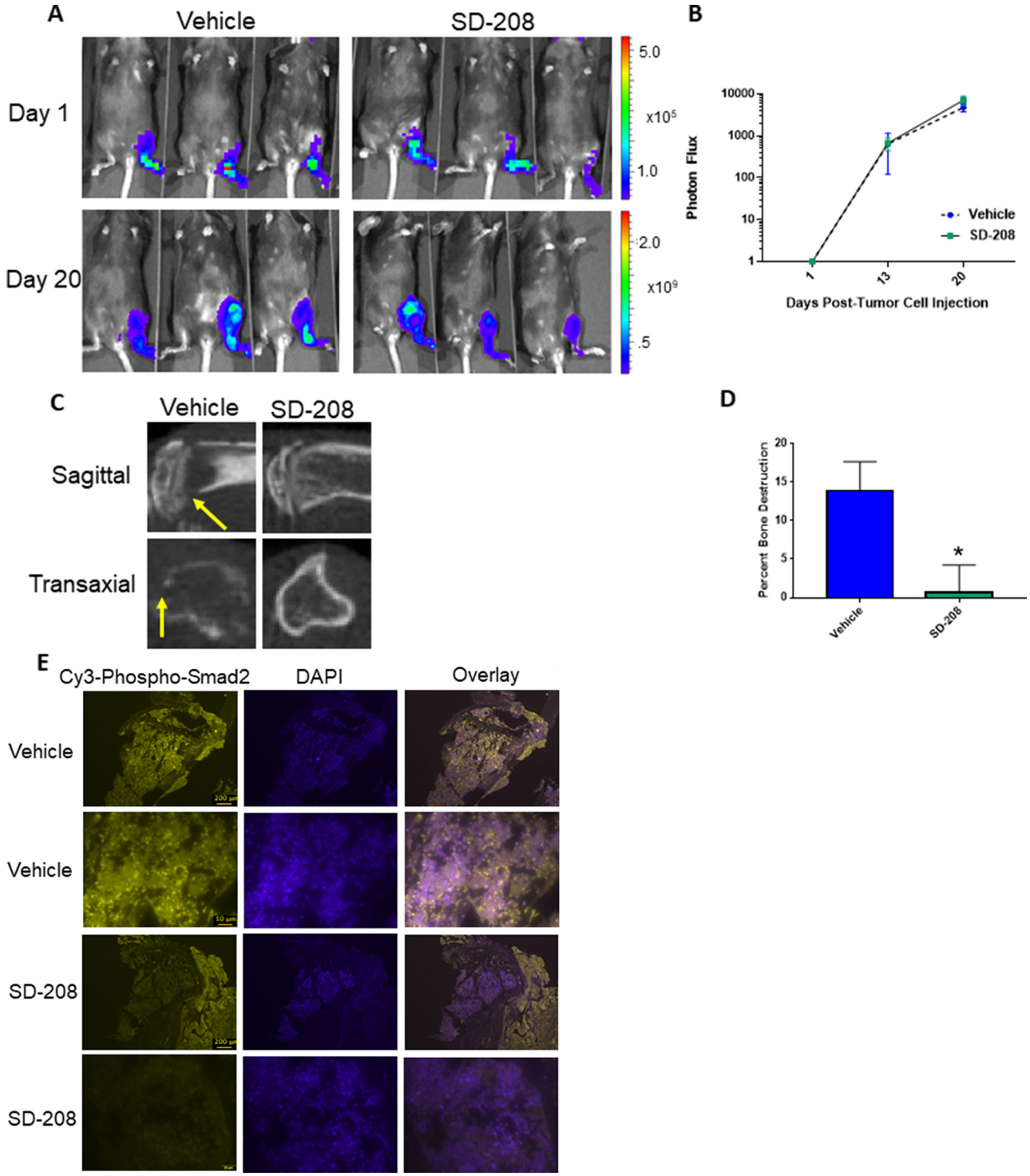

Figure 3. Inhibition of TGF-β signaling reduces osteolytic lesions in skeletally-immature female mice. Bioluminescent images of representative mice treated with SD-208 or vehicle control one and 20 d after injection of AT-3-FL cells via the left femoral artery. Scale bar shows pseudocolor display for photon flux values (A). Quantified bioluminescence data from mice in (A) shows equivalent growth of breast cancer cells in both groups. The graph shows mean values ± SEM (n = 4 mice per group) (B). Representative sagittal and transaxial CT images of proximal tibias of mice treated with SD-208 or vehicle at time of euthanization on day 19 (C). The yellow arrow shows osteolytic lesion. Quantified data for percent bone destruction in proximal tibias normalized to 0% on day 0 before injection (D). Treatment with SD-208 reduced bone destruction in proximal tibia of skeletally immature female mice (* denotes $P < .05$). Immunofluorescence images of phosphorylated Smad2 in proximal tibia of mice treated with SD-208 or vehicle control (E). Treatment with SD-208 blocked TGF-β activation of Smad2. DAPI depicts nucleated cells. Overlay shows active TGF-β signaling is from nucleated cells. Scale bars are as noted on images.

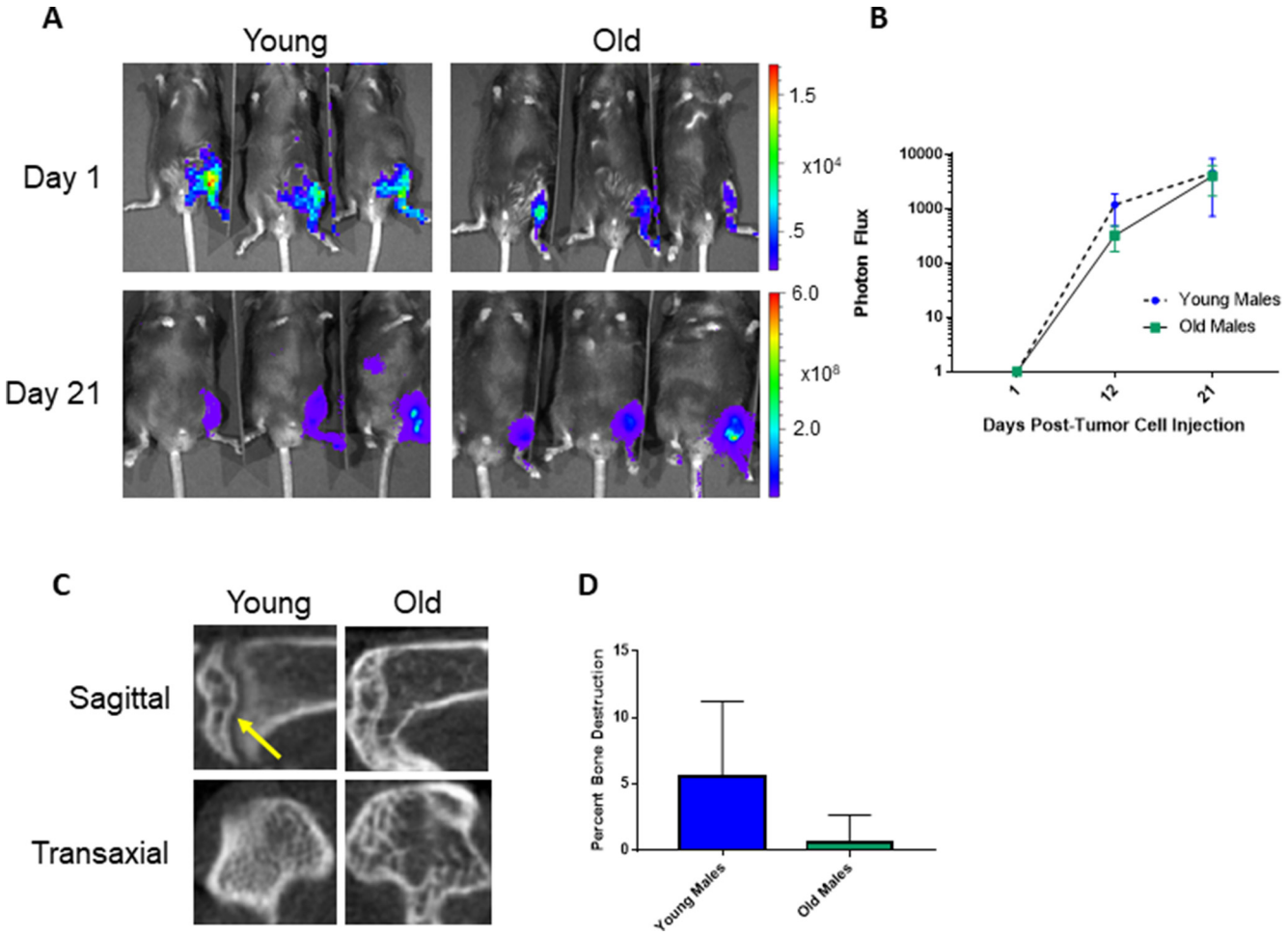

Figure 4. Male mice do not show age-dependent regulation of osteolytic metastases. Representative bioluminescence images of young (6–8 weeks) versus old (43–48 weeks) male mice 1 day and 21 days after injection of AT-3-FL cells via the left femoral artery. Scale bar depicts pseudocolor display for photon flux values (A). The graph of mean values ± SEM for bioluminescence imaging data shows no significant difference between the growth of cancer cells in the hind leg of skeletally mature and skeletally immature male mice (B). Sagittal and transaxial CT images of proximal tibias of young and old male mice show no bone destruction. Representative images of skeletally immature "young" and skeletally mature "old" proximal tibia at time of euthanization. The arrow shows open physis in a young male mouse (C). Quantified data (mean values + SEM) for percent bone destruction in proximal tibias of young and old male mice normalized to 0% before injection (day 0) (D). Both groups show comparable, minimal change in bone volume.

diac injection model (23). Because lower extremity physes do not close until mice reach 5 months of age (24), prior investigation still analyzed 2 cohorts of skeletally immature mice, likely underestimating protective effects of skeletal maturation against osteolytic metastases. Overall, the significant differences in osteolytic breast cancer metastases in young versus old mice emphasize the importance of age of experimental animals in preclinical models as a relevant biologic variable for studies of bone metastases in adult patients.

Although older mice show relative resistance to osteolytic breast cancer metastases, these animals still maintain normal levels of estrogen (25). Because most patients with breast cancer lack physiologic estrogen because of menopause or hormonal therapies, we surgically removed ovaries from mice to establish a more appropriate model system. Ovariectomy accelerates bone turnover and net loss of trabecular and cortical bone in mice, similar to effects in patients (26). Our data showed that ovariectomy increased susceptibility of older mice to osteolytic breast cancer metastases, although the extent of bone destruction in tibias remained less compared with younger animals. AT-3-FL breast cancer cells originated from a genetically engineered mouse breast cancer model that lacks estrogen receptor-α, so loss of estrogen did not affect proliferation of these cells in the bone environment of ovariectomized mice. Therefore, differences in disease progression arise from effects on bone and other components of the tumor environment. By establishing that ovariectomy promotes osteolytic metastasis in older mice, our results expand upon prior studies with skeletally immature mice showing

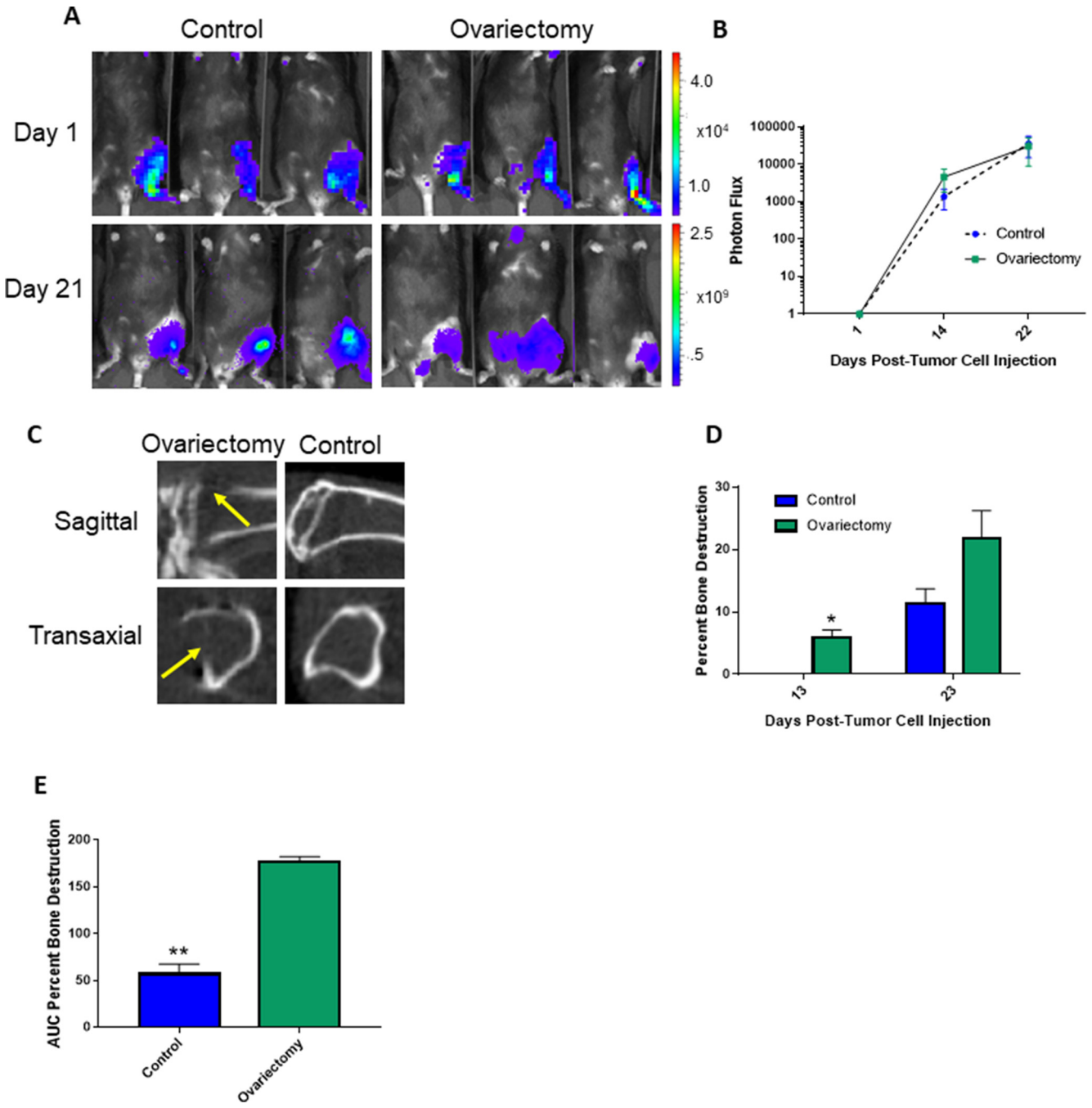

Figure 5. Ovariectomy increases osteolytic bone lesions in older female mice. Bioluminescence images of representative old (58–60 weeks) female mice that had undergone bilateral ovariectomy or sham surgery 5 weeks before left femoral artery injection of AT-3-FL breast cancer cells (A). The panel shows bioluminescence images of representative mice on 1 day and 21 days after injection with photon flux displayed as a pseudocolor scale of intensity values. Quantified data for growth of AT-3 breast cancer cells measured by bioluminescence imaging (n = 5 mice per group) reveal no difference between groups (B). The yellow arrows show foci of bone destruction in the proximal tibia of ovariectomized mice injected with AT-3-FL breast cancer cells (C). Graph shows mean values + SEM for percent bone destruction in proximal tibia relative to baseline (0%) image on day 0 before injection of breast cancer cells (D). Representative images of proximal tibia at time of euthanization (* denotes $P < .05$). Area-under-the-curve analysis of percent bone destruction calculated for both groups of mice over the full-time course after injection of breast cancer cells. ** denotes $P < .0001$ for greater bone destruction in the proximal tibia of ovariectomized mice (E).

that loss of anabolic bone hormones, such as estrogen and androgens, accelerates progression of bone metastases (24, 27, 28).

In addition to steroid hormones, other soluble molecules regulate the balance between bone formation or loss in normal physiology and metastasis. TGF-β is one of the most abundant cytokines in physes of skeletally immature mice and matrix of bone at all ages (29, 30). Signaling by TGF-β promotes bone destruction by blocking maturation of bone-forming osteoblasts and activating bone-resorbing osteoclasts. Within bone and bone marrow, disseminated cancer cells initiate osteoclast-mediated bone destruction, releasing TGF-β as part of an ongoing feed-forward loop to produce osteolytic metastases. Our experiments showed TGF-β as a key driver of bone destruction in the proximal tibia of young mice relative to old mice. Using phosphorylated SMAD2 as a marker of TGF-β signaling, we showed that young mice have notably higher activation of this pathway in proximal tibia. Furthermore, treatment with an inhibitor of TGF-β signaling, SD-208, reduced osteolytic lesions in young mice. SD-208 did not alter the proliferation of breast cancer cells in bone based on bioluminescence imaging, highlighting bone stromal cells as key targets of TGF-β signaling in bone metastases. Our experiments do not distinguish between TGF-β derived from the physis versus bone matrix, although both sources of this cytokine likely contribute to osteolysis in the proximal tibia. Clinical translation of TGF-β inhibitors remains challenging because of complex effects of this cytokine on cancer and stromal cells at different points in disease progression (31). Despite these challenges, our studies reinforce potential benefits of targeting this signaling pathway to reduce osteolytic bone metastases and associated complications.

Although TGF-β is present in the physes of both male and female mice, only female mice exhibited age-dependent differences in osteolytic metastasis in our model system. We found no difference in bone destruction when comparing young versus old male mice with ages comparable to female mice used in our studies, and minimal bone destruction occurred in either group of male mice. Because breast cancer occurs rarely in men, few data exist about the biology of metastasis and potential distinctions from the disease in women to establish to what extent our model reproduces human cancer. Elevated levels of estrogen significantly enhance risk for breast cancer in men, supporting the need for future studies to determine to what extent estrogen supplementation would increase osteolytic lesions in male mice. Independent of possible mechanisms, these data highlight the importance of investigating disease processes in both genders when relevant.

While bypassing early steps in spontaneous metastasis, the femoral artery injection model of experimental bone metastasis used in this research selectively disseminates cancer cells via a physiologic route to lower extremity bone marrow. This approach overcomes nonphysiological direct injection of cancer cells into the bone and the effects of systemic metastases generated by intracardiac injection. Despite the initial uniform distribution of cancer cells throughout femur and tibia following injection, we consistently observed preferential growth of breast cancer cells and osteolytic metastases in the proximal tibia. Tropism for the proximal tibia occurred in both young and old female mice, indicating that factors other than an open physis enhance the growth of breast cancer cells and associated bone destruction. Additional studies profiling heterogeneity of stromal cells and/or secreted molecules within subregions of bone and bone marrow will be required to understand the mechanisms driving metastasis in the proximal tibia versus other sites in the hind limb. Overall, this study demonstrates age- and gender-dependent effects on progression and extent of osteolytic bone metastases, emphasizing the importance of matching characteristics of the patient population of interest to a relevant model system. We expect the femoral artery injection model of bone metastasis described in this work will be an invaluable method to answer this and other challenges in bone metastasis and effects of therapy.

ACKNOWLEDGMENTS

We acknowledge research support from NIH grants R01CA196018, R01CA195655, and U01CA210152. We thank the Department of Radiology at The University of Michigan for the use of The Center for Molecular Imaging and The Preclinical Imaging & Computational Analysis Shared Resource, which are supported in part by Comprehensive Cancer Center NIH grant P30 CA046592.

Disclosures: The authors have nothing to disclose.

Conflict of Interest: None reported.

REFERENCES

1. Mariotto AB, Etzioni R, Hurlbert M, Penberthy L, Mayer M. Estimation of the number of women living with metastatic breast cancer in the United States. Cancer Epidemiol Biomarkers Prev. 2017;26:809–815.
2. Chen L, Linden HM, Anderson BO, Li CI. Trends in 5-year survival rates among breast cancer patients by hormone receptor status and stage. Breast Cancer Res Treat. 2014;147:609–616.
3. Howlader N, Noone AM, Krapcho M, Miller D, Bishop K, Kosary CL, Yu M, Ruhl J, Tatalovich Z, Mariotto A, Lewis DR, Chen HS, Feuer EJ, Cronin KA (eds). SEER Cancer Statistics Review, 1975-2014, National Cancer Institute. Bethesda, MD. Available at: https://seer.cancer.gov/csr/1975_2014/ based on November 2016 SEER data submission, posted to the SEER web site, April 2017 (2017).
4. Jingushi S, Scully SP, Joyce ME, Sugioka Y, Bolander ME. Transforming growth factor-beta 1 and fibroblast growth factors in rat growth plate. J Orthop Res. 1995;13:761–768.
5. Jilka RL. The relevance of mouse models for investigating age-related bone loss in humans. J Gerontol A Biol Sci Med Sci. 2013;68:1209–1217.
6. van Staa TP, Dennison EM, Leufkens HG, Cooper C. Epidemiology of fractures in England and Wales. Bone. 2001;29:517–522.
7. Campbell JP, Merkel AR, Masood-Campbell SK, Elefteriou F, Sterling JA. Models of bone metastasis. J Vis Exp. 2012;67:e4260.
8. Hibberd C, Cossigny DA, Quan GM. Animal cancer models of skeletal metastasis. Cancer Growth Metastasis. 2013;6: 23–34.
9. Wang H, Yu C, Gao X, Welte T, Muscarella AM, Tian L, Zhao H, Zhao Z, Du S, Tao J, Lee B, Westbrook TF, Wong ST, Jin X, Rosen JM, Osborne CK, Zhang XH. The osteogenic niche promotes early-stage bone colonization of disseminated breast cancer cells. Cancer Cell. 2015;27:193–210.
10. Fenner J, Stacer AC, Winterroth F, Johnson TD, Luker KE, Luker GD. Macroscopic stiffness of breast tumors predicts metastasis. Sci Rep. 2014;4:5512.
11. Luker KE, Lewin SA, Mihalko LA, Schmidt BT, Winkler JS, Coggins NL, Thomas DG, Luker GD. Scavenging of CXCL12 by CXCR7 promotes tumor growth and metastasis of CXCR4-positive breast cancer cells. Oncogene. 2012;31:4750–4758.

12. Ström JO, Theodorsson A, Ingberg E, Isaksson IM, Theodorsson E. Ovariectomy and 17β-estradiol replacement in rats and mice: a visual demonstration. J Vis Exp. 2012;e4013.
13. Smith MC, Luker KE, Garbow JR, Prior JL, Jackson E, Piwnica-Worms D, Luker GD. CXCR4 regulates growth of both primary and metastatic breast cancer. Cancer Res. 2004;64:8604–8612.
14. Brisset JC, Hoff BA, Chenevert TL, Jacobson JA, Boes JL, Galbán S, Rehemtulla A, Johnson TD, Pienta KJ, Galbán CJ, Meyer CR, Schakel T, Nicolay K, Alva AS, Hussain M, Ross BD. Integrated multimodal imaging of dynamic bone-tumor alterations associated with metastatic prostate cancer. PLoS One. 2015;10:e0123877.
15. Mohammad KS, Chen CG, Balooch G, Stebbins E, McKenna CR, Davis H, Niewolna M, Peng XH, Nguyen DH, Ionova-Martin SS, Bracey JW, Hogue WR, Wong DH, Ritchie RO, Suva LJ, Derynck R, Guise TA, Alliston T. Pharmacologic inhibition of the TGF-beta type I receptor kinase has anabolic and anti-catabolic effects on bone. PLoS One. 2009;4:e5275.
16. Guise TA, Yin JJ, Taylor SD, Kumagai Y, Dallas M, Boyce BF, Yoneda T, Mundy GR. Evidence for a causal role of parathyroid hormone-related protein in the pathogenesis of human breast cancer-mediated osteolysis. J Clin Invest. 1996;98:1544–1549.
17. Bendre MS, Margulies AG, Walser B, Akel NS, Bhattacharrya S, Skinner RA, Swain F, Ramani V, Mohammad KS, Wessner LL, Martinez A, Guise TA, Chirgwin JM, Gaddy D, Suva LJ. Tumor-derived interleukin-8 stimulates osteolysis independent of the receptor activator of nuclear factor-kappaB ligand pathway. Cancer Res. 2005;65:11001–11009.
18. Zheng Y, Zhou H, Modzelewski JR, Kalak R, Blair JM, Seibel MJ, Dunstan CR. Accelerated bone resorption, due to dietary calcium deficiency, promotes breast cancer tumor growth in bone. Cancer Res. 2007;67:9542–9548.
19. Bonewald LF, Mundy GR. Role of transforming growth factor-beta in bone remodeling. Clin Orthop Relat Res. 1990;261–276.
20. Meng X, Vander Ark A, Lee P, Hostetter G, Bhowmick NA, Matrisian LM, Williams BO, Miranti CK, Li X. Myeloid-specific TGF-β signaling in bone promotes basic-FGF and breast cancer bone metastasis. Oncogene. 2016;35:2370–2378.
21. Uhl M, Aulwurm S, Wischhusen J, Weiler M, Ma JY, Almirez R, Mangadu R, Liu YW, Platten M, Herrlinger U, Murphy A, Wong DH, Wick W, Higgins LS, Weller M. SD-208, a novel transforming growth factor beta receptor I kinase inhibitor, inhibits growth and invasiveness and enhances immunogenicity of murine and human glioma cells in vitro and in vivo. Cancer Res. 2004;64:7954–7961.
22. Mak IW, Evaniew N, Ghert M. Lost in translation: animal models and clinical trials in cancer treatment. Am J Transl Res. 2014;6:114–118.
23. Wang N, Reeves KJ, Brown HK, Fowles AC, Docherty FE, Ottewell PD, Croucher PI, Holen I, Eaton CL. The frequency of osteolytic bone metastasis is determined by conditions of the soil, not the number of seeds; evidence from in vivo models of breast and prostate cancer. J Exp Clin Cancer Res. 2015;34:124.
24. Silbermann M, Kadar T. Age-related changes in the cellular population of the growth plate of normal mouse. Acta Anat (Basel). 1977;97:459–468.
25. Parkening TA, Lau IF, Saksena SK, Chang MC. Circulating plasma levels of pregnenolone, progesterone, estrogen, luteinizing hormone, and follicle stimulating hormone in young and aged C57BL/6 mice during various stages of pregnancy. J Gerontol. 1978;33:191–196.
26. Bouxsein ML, Myers KS, Shultz KL, Donahue LR, Rosen CJ, Beamer WG. Ovariectomy-induced bone loss varies among inbred strains of mice. J Bone Miner Res. 2005;20:1085–1092.
27. Ottewell PD, Wang N, Brown HK, Reeves KJ, Fowles CA, Croucher PI, Eaton CL, Holen I. Zoledronic acid has differential antitumor activity in the pre- and postmenopausal bone microenvironment in vivo. Clin Cancer Res. 2014;20:2922–2932.
28. Ottewell PD, Wang N, Brown HK, Reeves KJ, Fowles CA, Croucher PI, Eaton CL, Holen I. Castration-induced bone loss triggers growth of disseminated prostate cancer cells in bone. Endocr Relat Cancer. 2014;21:769–781.
29. Chiechi A, Waning DL, Stayrook KR, Buijs JT, Guise TA, Mohammad KS. Role of TGF-β in breast cancer bone metastases. Adv Biosci Biotechnol. 2013;4:15–30.
30. Wu M, Chen G, Li YP. TGF-β and BMP signaling in osteoblast, skeletal development, and bone formation, homeostasis and disease. Bone Res. 2016;4:16009.
31. Katz LH, Li Y, Chen JS, Muñoz NM, Majumdar A, Chen J, Mishra L. Targeting TGF-beta signaling in cancer. Expert Opin Ther Targets. 2013;17:743–760.